

See discussions, stats, and author profiles for this publication at: <https://www.researchgate.net/publication/6122945>

Distinctive Unimolecular Gas-Phase Reactivity of $[M(en)_2]^{2+}$ ($M = Ni, Cu$) Dications and Their Inclusion Complexes with the Macrocyclic Cavitand Cucurbit[8]uril

ARTICLE in JOURNAL OF THE AMERICAN SOCIETY FOR MASS SPECTROMETRY · NOVEMBER 2007

Impact Factor: 2.95 · DOI: 10.1016/j.jasms.2007.07.020 · Source: PubMed

CITATIONS

20

READS

57

5 AUTHORS, INCLUDING:



V. P. Fedin

Russian Academy of Sciences

442 PUBLICATIONS 5,357 CITATIONS

SEE PROFILE



Rosa Llusar

Universitat Jaume I

165 PUBLICATIONS 2,994 CITATIONS

SEE PROFILE



Ivan Sorribes

Leibniz Institute for Catalysis

23 PUBLICATIONS 312 CITATIONS

SEE PROFILE

Distinctive Unimolecular Gas-Phase Reactivity of $[M(en)_2]^{2+}$ ($M = Ni, Cu$) Dications and Their Inclusion Complexes with the Macrocyclic Cavitand Cucurbit[8]uril

Tatyana Mitkina,^a Vladimir Fedin,^a Rosa Llusar,^b Ivan Sorribes,^b and Cristian Vicent^c

^a A. V. Nikolaev Institute of Inorganic Chemistry, Siberian Branch of the Russian Academy of Sciences, Novosibirsk, Russian Federation

^b Departament de Química Física i Analítica, Universitat Jaume I, Castelló, Spain

^c Serveis Centrals d'Instrumentació Científica, Universitat Jaume I, Castelló, Spain

Electrospray ionization mass spectrometry makes it possible to generate gas-phase bis-ethylenediamine nickel and copper dications, $[M(en)_2]^{2+}$ ($M = Ni, 1; M = Cu, 2$), as well as their $\{[M(en)_2]@cuc[8]\}^{2+}$ inclusion complexes with the macrocyclic cavitand cucurbit[8]uril (cuc[8]). The unimolecular gas-phase reactivity of these species has been investigated by electrospray ionization tandem mass spectrometry with a quadrupole-time-of-flight configuration. Distinctive fragmentation pathways have been observed for the free and encapsulated $[M(en)_2]^{2+}$ ($M = Ni, Cu$) dications under collision-induced dissociation (CID) conditions. The dications $[M(en)_2]^{2+}$ ($M = Ni, Cu$) dissociate according to several competitive pathways that involve intra-complex hydrogen or electron-transfer processes. Most of these channels are suppressed after encapsulation inside the cucurbit[8]uril macrocycle and, as a consequence, a simplification of the $\{[M(en)_2]@cuc[8]\}^{2+}$ fragmentation pattern is observed. The results obtained demonstrate that the encapsulation of a coordination complex inside a host molecule can be used to alter the nature of the product ions generated under CID conditions. (J Am Soc Mass Spectrom 2007, 18, 1863–1872) © 2007 American Society for Mass Spectrometry

The research on the noncovalent interactions in the host-guest chemistry has benefited greatly from the latest advances in soft-ionization mass spectrometric techniques. The development of the mass spectrometry methods over the past years made it possible to qualitatively and quantitatively evaluate host binding selectivities, relative binding constants of host-guest complexes, and to get a deeper insight into the principles of molecular recognition phenomena. These achievements are illustrated in numerous gas-phase ion chemistry investigations on various host-guest aggregates with such host molecules as cyclodextrins [1], crown-ethers [2], calixarenes [3, 4], and resorcinarenes [5]. One more host system that has proven to encapsulate a wide range of guest molecules is that of cucurbit[*n*]uril (where *n* usually varies from 5 to 8). Cucurbit[*n*]urils form a family of macrocyclic barrel-shaped molecules having rather rigid structures built by *n* glycoluril units connected via methylene bridging groups (Chart 1). These macrocycles have a hydrophobic cavity with approximate diameter of 9 Å for cucurbit[8]uril and this cavity can be accessed

through two identical carbonyl-fringed portals. The variability of the cavity and portal dimensions creates a basis for molecular recognition displayed by these host systems, the feature making them very attractive [6–8].

Encapsulation of guest species by a host molecule can substantially affect some fundamental properties of the encapsulated species such as their geometry, thermal stability, magnetism, photo- and electrochemistry, as well as reactivity. For the case of cucurbit[*n*]urils, supramolecular aggregates of the host receptors with bare cations, organic molecules and inorganic complexes are known and their properties have been thoroughly investigated using solid-state and solution methods. In contrast, gas-phase studies in cucurbit[*n*]urils host-guest chemistry are relatively scarce despite the fact that mass spectrometry is used routinely to characterize this class of compounds [9]. To the best of our knowledge, the only two reports on this topic came from Dearden's group. One of them deals with the encapsulation of N_2 , O_2 , CH_3OH and CH_3CN by the {decamethylcucurbit [5]uril}(NH_4^+)₂ adduct [10]. The other has to do with the gas-phase generation of 1:1 aggregates formed by the cucurbit [6]uril homologue and diamines, with a pseudorotaxane disposition [11]. In both cases, the electrospray ionization has been used as an ionization technique.

Address reprint requests to Dr. C. Vicent, Serveis Centrals d'Instrumentació Científica, Universitat Jaume I-Campus de Riu Sec, 12071 Castellón, Spain. E-mail: barrera@sg.uji.es

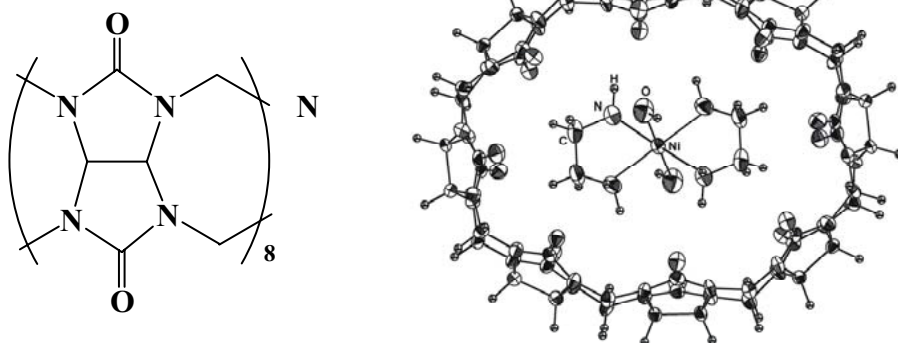


Chart 1

In general, the gas-phase studies of host-guest complexes are restricted to the systems with small biomolecules or bare cations as guest components and little attention has been paid to the encapsulation of coordination complexes. One of the largest members of the cucurbit[n]uril family, cucurbit[8]uril, has proved to encapsulate cobalt, nickel, copper and zinc complexes with aliphatic polyamine ligands such as ethylenediamine, cyclam, or cyclen (cyclam = 1,4,8,11-tetraazacyclotetradecane; cyclen = 1,4,7,10-tetraazacyclododecane), although no gas-phase studies on the host-guest complexes have been reported so far [12–15]. This fact is in contrast with numerous gas-phase ion chemistry studies on non-encapsulated polyamine transition-metal complexes as, for example, $[M(\text{cyclam})]^{2+}$ ($M = \text{Ni}, \text{Cu}$) [16], diethylenetriamine derivatives coordinated to copper [17], or the ethylenediamine complexes $[\text{Ni}(\text{en})_n]^{2+}$ ($n = 2\text{--}5$) [18] and $[\text{Cu}(\text{en})]^{+}$ [19]. In particular, the studies on the diethylenetriamine or 2,2':6',2'-terpyridine complexes of copper have been primarily motivated by the ability of these complexes to bind small biomolecules (such as amino acids or nucleic acids) and subsequently generate the corresponding radical cations under CID conditions [20–23].

In the past years, many efforts have been applied to fine-tune the electronic properties of coordination complexes, especially by varying the nature of the ancillary ligands or the metal [23–25] to promote and/or control the formation of desired organic radical cations. In this context, an alternative way to selectively direct the fragmentation of the target complex would be the inclusion of such complexes inside a host. In this scenario, the restriction of the guest's intramolecular rotational mobility within the cavity could direct the fragmentation of a host-guest complex towards product ions different from those observed for the free transition complex under CID conditions.

To validate this approach, we report here a gas-phase study of the dications $[\text{M}(\text{en})_2]^{2+}$ ($M = \text{Ni}, \text{Cu}$) and their inclusion complexes $\{[\text{M}(\text{en})_2]@ \text{cuc}[8]\}^{2+}$ (where $M = \text{Ni}, \text{Cu}$; en = ethylenediamine) generated by electrospray ionization mass spectrometry. An

ORTEP representation of the X-ray crystal structure of the encapsulated $\{trans\text{-}[\text{Ni}(\text{en})_2(\text{H}_2\text{O})_2]@ \text{cuc}[8]\}^{2+}$ dication is shown in Chart 1 to illustrate its main geometric features.

Experimental

The mononuclear complexes $\{trans\text{-}[\text{Ni}(\text{en})_2\text{Cl}_2]\}$, $[\text{Cu}(\text{en})_2]\text{Cl}_2 \cdot 0.5\text{H}_2\text{O}$ and their inclusion compounds $\{trans\text{-}[\text{Ni}(\text{en})_2(\text{H}_2\text{O})_2]@ \text{cuc}[8]\}\text{Cl}_2 \cdot 23.5\text{H}_2\text{O}$, $\{trans\text{-}[\text{Cu}(\text{en})_2(\text{H}_2\text{O})_2]@ \text{cuc}[8]\}\text{Cl}_2 \cdot 17\text{H}_2\text{O}$ were prepared according to the literature procedures [13, 14]. A hybrid QTOF I (quadrupole-hexapole-time-of-flight) mass spectrometer with an orthogonal Z-spray-electrospray interface (Micromass, Manchester, UK) was utilized. Nitrogen was used as a drying gas and as nebulizing gas at a flow of 600 L/h and 20 L/h, respectively. The temperature of the source block was set to 120 °C and the desolvation temperature to 150 °C. Mass calibration was performed using a solution of sodium/cesium iodide in isopropanol:water (50:50) from m/z 30 to 2000. Gas-phase generation of the dications $[\text{M}(\text{en})_2]^{2+}$ and $\{[\text{M}(\text{en})_2]@ \text{cuc}[8]\}^{2+}$ ($M = \text{Ni}, \text{Cu}$) was carried out by electrospraying 5×10^{-4} M solutions of the desired compound. Preparation of the amine groups deuterated homologues was achieved by incubation of the corresponding starting materials in deuterated methanol/water or deuterated water solutions for 12 h. The ESI mass spectra of these deuterated homologues were recorded in $\text{CD}_3\text{OD}/\text{D}_2\text{O}$ mixtures or D_2O to avoid H/D exchange. The capillary voltage was set at 3.5 kV in the positive scan mode and the cone voltage was adjusted (typically U_c 15 to 35 V) to maximize ion abundances of the target ions and control the extent of fragmentation in the source region. Sample solutions were infused via syringe pump directly connected to the ESI source at a flow rate of 10 $\mu\text{L}/\text{min}$. The observed isotopic pattern of each species perfectly matched the theoretical isotope pattern calculated from their elemental composition using the MassLynx 4.0 program. Tandem MS/MS spectra were obtained at various collision energies (typically varied from $E_{\text{lab}} =$

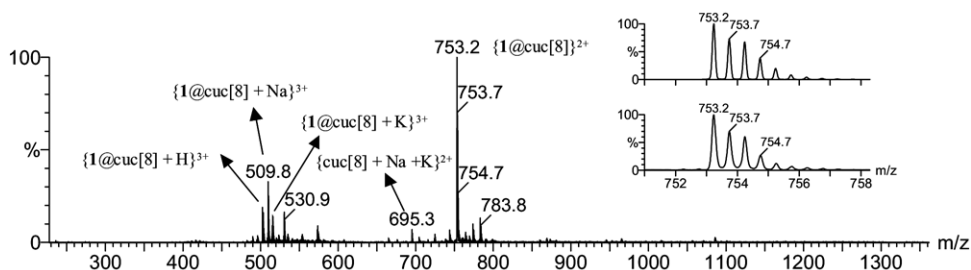


Figure 1. Electrospray mass spectrum of 5×10^{-4} M aqueous solutions of the compound $\{trans\text{-}[\text{Ni}(\text{en})_2(\text{H}_2\text{O})_2]@\text{cuc}[8]\}\text{Cl}_2 \cdot 23.5\text{H}_2\text{O}$ recorded at cone voltage $U_c = 20$ V. The inset shows the experimental (bottom) and calculated (top) isotope patterns for $\{1@\text{cuc}[8]\}^{2+}$.

0 to 50 eV) by selecting the precursor ion of interest with the first quadrupole (Q1) and interaction with argon in the hexapole cell while mass analyzing the products with the time of flight analyzer (TOF). An isolation width of ~ 1 Da was used. Argon was used as a collision gas to produce the pressure of 3×10^{-5} mbar as measured in the quadrupole analyzer region. Some product ions in the CID spectra of the 1^{2+} and 2^{2+} dications were tentatively assigned to water-containing species arising from bimolecular reactions with background water present in the collision cell of the Q-TOF instrument.

Results and Discussion

ESI-MS and ESI-MS/MS of $\{[\text{Ni}(\text{en})_2]@\text{cuc}[8]\}^{2+}$ ($\{1@\text{cuc}[8]\}^{2+}$) and $[\text{Ni}(\text{en})_2]^{2+}$ (1^{2+}) Dications

The ESI mass spectrum of aqueous solutions of the compound $\{trans\text{-}[\text{Ni}(\text{en})_2(\text{H}_2\text{O})_2]@\text{cuc}[8]\}\text{Cl}_2 \cdot 23.5\text{H}_2\text{O}$ recorded at cone voltage $U_c = 20$ V is shown in Figure 1. The spectrum reveals the presence of the dicationic species $\{[\text{Ni}(\text{en})_2]@\text{cuc}[8]\}^{2+}$ ($\{1@\text{cuc}[8]\}^{2+}$), as the base peak, together with a set of triply charged ions assigned to the protonated, sodium and potassium adducts of general formula $\{1@\text{cuc}[8] + \text{Y}\}^{3+}$ ($\text{Y} = \text{H}, \text{Na}, \text{K}$).

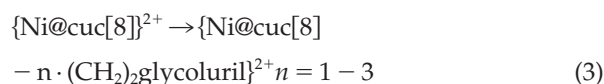
The use of low cone voltages (typically below $U_c = 10$ V) produces cations formed by the coordination of one or two water molecules, with formula $\{[\text{H}_2\text{O}]_n@\text{cuc}[8]\}^{2+}$, and lower ion abundances for the species of interest, namely $\{1@\text{cuc}[8]\}^{2+}$. Maximum ion abundances for this dication are achieved at $U_c = 20$ V. It has to be pointed out that peaks corresponding to the macrocycle or the guest complex are only observed as minor signals under these conditions, thus suggesting that the supramolecular aggregate $\{1@\text{cuc}[8]\}^{2+}$ is not prone to dissociate, neither in solution nor in gas phase. These preliminary single-stage ESI-MS experiments indicate that the gas-phase $\{1@\text{cuc}[8]\}^{2+}$ dications are stable enough to survive the electrospray ionization process and suggest the presence of an inclusion complex in the gas phase.

Electrospraying a water:methanol (50:50) solution of the complex $[\text{trans}\text{-}\text{Ni}(\text{en})_2\text{Cl}_2]$ produces the $[\text{Ni}(\text{en})_2]^{2+}$ (1^{2+}) dication as well as the singly-charged $[\text{Ni}(\text{en})_2 -$

$\text{H}]^+$ and $[\text{Ni}(\text{en})_2 + \text{Cl}]^+$ species. The use of different cone voltages significantly changes the relative intensity of the species detected. At low cone voltages ($U_c = 15$ V), the $[\text{Ni}(\text{en})_2 + \text{Cl}]^+$ and $[\text{Ni}(\text{en})_2]^{2+}$ species dominate, while at higher cone voltages (typically $U_c = 35$ V) the $[\text{Ni}(\text{en})_2 - \text{H}]^+$ species are seen as the base peak. Maximum abundances for the 1^{2+} dication are observed at $U_c = 15$ V. Similar ionization pattern has been reported for the family of nickel complexes $[\text{Ni}(\text{cyclam})]^{2+}$ with different anions, where the peaks of $[\text{Ni}(\text{cyclam})]^{2+}$, $[\text{Ni}(\text{cyclam}) - \text{H}]^+$, and $[\text{Ni}(\text{cyclam}) + \text{X}]^+$ were dominant in the ESI spectra [16].

In this work, we will focus on the comparison of the unimolecular dissociation of the dications 1^{2+} in two different gas-phase environments ("free" and encapsulated within the cucurbit[8]uril cavity). For this purpose, we have investigated the CID spectra of these species while increasing collision energies. In these experiments, the doubly-charged ions were separated by their mass-to-charge ratio, accelerated into the collision cell of the mass spectrometer and subsequently analyzed with the time-of-flight analyzer. The CID mass spectra of the mass-selected $\{1@\text{cuc}[8]\}^{2+}$ ion have been recorded covering the range $E_{\text{lab}} = 0$ to 50 eV. Figure 2 shows two representative CID spectra at $E_{\text{lab}} = 20$ (bottom) and 40 eV (top) for the $\{1@\text{cuc}[8]\}^{2+}$ dication.

Similar experiments were carried out selecting the complete cluster peak to establish the elemental composition of the product ions. In general, the analysis of the isotopic pattern of the product ions indicates that peaks above 400 Th correspond to nickel-containing species while ions observed at lower mass-to-charge ratios correspond to species containing [C, H, N, O]. The fragmentation pathways for the $\{1@\text{cuc}[8]\}^{2+}$ dication are represented schematically by eqs 1 to 3:



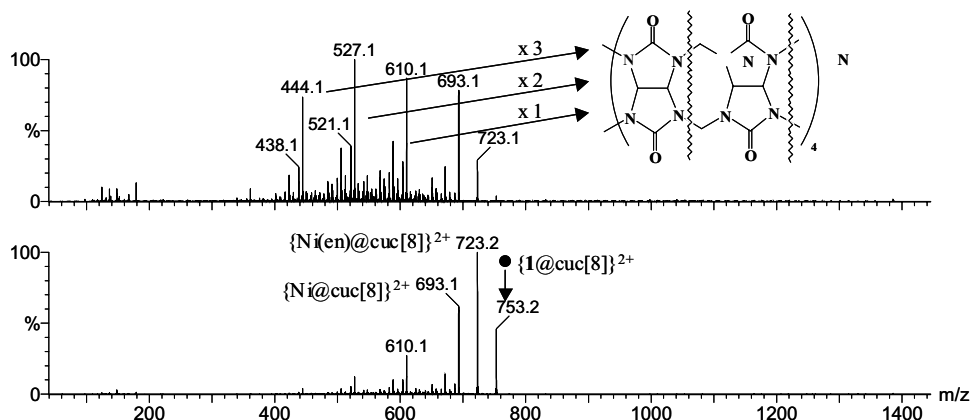


Figure 2. Fragment ions formed upon CID of the mass-selected species $\{1@cuc[8]\}^{2+}$ at $m/z = 753.3$ Th, at $E_{lab} = 20$ eV (bottom) and $E_{lab} = 40$ eV (top).

At low collision energies (below $E_{lab} = 10$ eV) (spectra not shown), mass-selected dication $\{1@cuc[8]\}^{2+}$ ($m/z = 753.2$ Th) generates product ions through bimolecular reactions with adventitious water available in the collision cell (peak at $m/z = 762.2$ Th, $\{[1(H_2O)]@cuc[8]\}^{2+}$). At collision energies close to $E_{lab} = 20$ eV, subsequent evaporation of two neutral ethylenediamine molecules yields $\{Ni(en)@cuc[8]\}^{2+}$ ($m/z = 723.2$ Th) and $\{Ni@cuc[8]\}^{2+}$ ($m/z = 693.1$ Th) species. Gradual increase of the collision energy (up to $E_{lab} = 50$ eV) causes increasing loss of the ligand and the expulsion of up to three neutral fragments to generate peaks at $m/z = 610.1$, 527.1 and 444.1 Th. These fragments most likely result from the loss of one or more bis-N-methylene-glycoluril subunits of the formula $C_6N_4O_2H_6$. The formation of such fragment may occur through four C–N cleavages as shown schematically in Figure 2. Other minor fragmentation channels are also observed which most likely arise from complex rearrangement processes on the macrocycle. Under these conditions, severe attenuation of the whole ion signal was observed, thus suggesting that the ejection of the precursor ion from the hexapole is competitive with the CID process.

It is well-documented that the gas-phase structure elucidation of host-guest systems after the ESI process is not trivial as non-specific electrostatic adducts cannot be clearly distinguished from inclusion complexes. In this regard, a great deal of work has been reported on the identity of noncovalent complexes formed between cyclodextrins and various guest molecules [1, 26]. One way to verify whether the observed species in the gas-phase are real inclusion complexes consists in examining their decomposition under collision-induced dissociation conditions [27, 28]. Fragmentation of the guest molecule while retaining the macrocycle should be observed in those species which possess an encapsulated guest. In the present case, clearly neither the 1^{2+} dication nor species arising from the free cucurbit[8]uril macrocycle were observed as product ions. This observation confirms that $\{1@cuc[8]\}^{2+}$ is a real inclusion complex in the gas-phase. This fact provides a unique

opportunity to determine the effect of encapsulation on the characteristic unimolecular dissociation of the 1^{2+} dication.

The gas-phase dissociation of the 1^{2+} dication reveals complex rearrangement pathways that include intra-complex hydrogen and electron-transfer processes. In addition to these competitive fragmentations channels, other product ions have been found and tentatively assigned to bimolecular reactions with background water available in the collision cell of the Q-TOF instrument, the resulting CID spectra being very crowded. The presence of the water adducts was further supported while using CD_3OD/D_2O mixtures as a solvent. Figure 3 shows the CID spectra recorded at $E_{lab} = 10$ and 15 eV for mass-selected 1^{2+} species.

Most of the product ions formed from the doubly-charged 1^{2+} dication are singly-charged ions, where the nickel atom remains coordinated to one of the organic ligands and to a part of the ligand, or only to one part of the ligand. The product ions that retain nickel are clearly distinguished in the CID experiments upon mass-selection of the less abundant ^{60}Ni -containing precursor isotopomer. Fragmentation of 1^{2+} starts at low collision energies (see Figure 3 bottom) and generates various major product ions whose molecular composition is shown in Figure 3.

In closely related doubly charged transition-metal complex $[ML_n]^{2+}$ ions (where L stands for protic and aprotic ligands such as water [29, 30], acetamide [31], dimethylsulfoxide [29, 32], or acetonitrile [33, 34], ligand-to-metal electron transfers are typically energetically favorable once a critical ion size has been reached. This is due to the lower ionization energy of the ligands as compared to the high second ionization energy of the metal. In the case of protic ligands, intra-complex hydrogen transfer can also readily take place resulting in a charge reduction as well. Both processes are observed for the 1^{2+} dication together with the heterolytic rupture of the ethylenediamine molecule according to eqs 4, 5, 6, and 7:

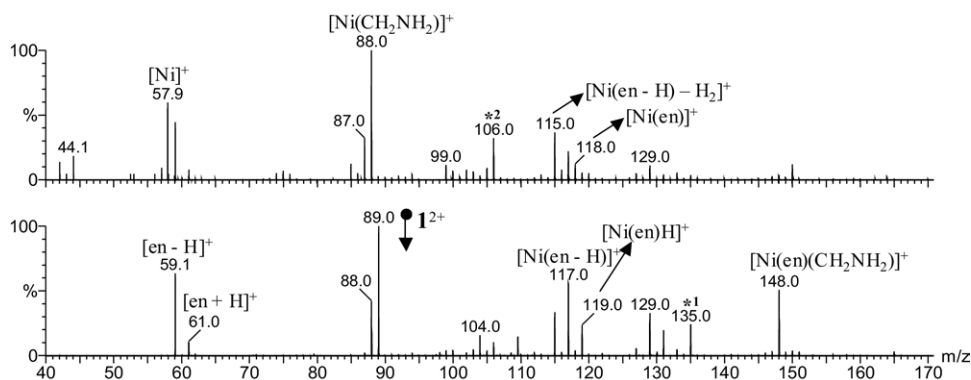
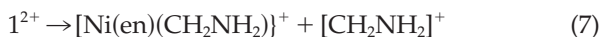
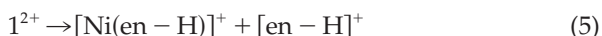
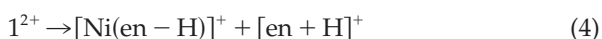


Figure 3. Fragment ions formed upon CID of mass-selected species 1^{2+} at $m/z = 89.0$ Th, at $E_{\text{lab}} = 10$ eV (bottom) and $E_{\text{lab}} = 15$ eV (top). Peaks marked with an asterisk correspond to product ions produced in bimolecular reactions with water: $^{*1}[\text{Ni}(\text{en} - \text{H}) + \text{H}_2\text{O}]^+$ at $m/z = 135.0$ Th and $^{*2}[\text{Ni}(\text{CH}_2\text{NH}_2) + \text{H}_2\text{O}]^+$ at $m/z = 106.0$ Th.



Eq 4 generates the species $[\text{Ni}(\text{en} - \text{H})]^+$ at $m/z = 117.0$ Th and $[\text{en} + \text{H}]^+$ at $m/z = 61.1$ Th through an inter-ligand proton transfer followed by charge splitting. CID experiments using deuterated ethylenediamine ($\text{ND}_2\text{CH}_2\text{CH}_2\text{ND}_2$ or $\text{d}_4\text{-en}$) were carried out to reveal that the proton loss takes place on one of the amine groups. Similar fragmentation involving inter-ligand proton transfer has been reported for the $[\text{Ni}(\text{en})_3]^{2+}$ species, which produces $[\text{Ni}(\text{en})(\text{en} - \text{H})]^{2+}$ and $[\text{en} + \text{H}]^+$ [18].

Another channel, represented by eq 5, may involve hydride migration from one organic ligand to the nickel site followed by charge splitting to produce $[\text{Ni}(\text{en}) + \text{H}]^+$ ($m/z = 119.0$ Th) and deprotonated ethylenediamine $[\text{en} - \text{H}]^+$ at $m/z = 59.1$ Th. This process was confirmed by the use of $\text{d}_4\text{-en}$ that revealed hydrogen migration occurring from the methylene group of *en*; therefore, the presence of a hydride intermediate can be reasonably postulated. The presence of metal hydride species has been reported previously in the CID spectra of several alkylamine copper complexes, namely $[\text{Cu}(\text{en})]^+$ and $[\text{Cu}(\text{R}_2\text{-dien})]^{2+}$ (where $\text{R}_2\text{-dien}$ stands for disubstituted diethylenetriamine) [17, 19, 35]. In the case of $[\text{Cu}(\text{en})]^+$, theoretical calculations and deuterium labeling experiments suggest that hydrogen abstraction takes place from the ethylene chain, while for $[\text{Cu}(\text{R}_2\text{-dien})]^{2+}$ complexes the hydrogen atom originates from the amine. The presence of hydride species in the gas-phase has also been observed for methanol complexes of Co, Mn and Zn as a result of hydride transfer processes upon CID conditions [36, 37]. In the

case of the $[\text{M}(\text{CH}_3\text{OH})_4]^{2+}$ dications ($\text{M} = \text{Co}, \text{Mn}$), their gas-phase dissociation reveals the presence of competitive fragmentation pathways involving proton and hydride transfer, similar to that found for the 1^{2+} dication [36].

Intra-complex electron-transfer followed by charge separation according to eq 6 might account for the appearance of $[\text{Ni}(\text{en})]^+$ cation at $m/z = 118.0$ Th and non-detected $-^+$ species, presumably due to their further fragmentation to afford cations with lower mass-to-charge ratios. Eq 7 generates the nickel-containing cation $[\text{Ni}(\text{en})(\text{CH}_2\text{NH}_2)]^+$ ($m/z = 148.0$ Th) through the heterolytic cleavage of a carbon-carbon bond, and the immonium $[\text{CH}_2 = \text{NH}_2]^+$ cation.

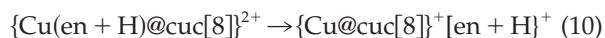
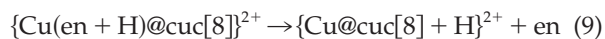
Other nickel-containing fragments formed with the release of neutral H_2 , NH_3 , or $\text{CH}_2 = \text{NH}_2$ molecules are simultaneously observed along with the mentioned product ions. In the lower mass-to-charge region, peaks containing {C, N, H} are also observed (at $m/z = 42.0$ and 44.0 Th) and attributed to rearrangement processes of the organic ligand. Most of the ions are produced by consecutive fragmentations of other product ions. For example, gas-phase generation of species $[\text{Ni}(\text{en})(\text{CH}_2\text{NH}_2)]^+$ at $m/z = 148.0$ was achieved by “in-source” fragmentation of 1^{2+} at higher cone voltages (typically in the range $U_c = 40$ to 60 V). Mass-selection and dissociation of the $[\text{Ni}(\text{en})(\text{CH}_2\text{NH}_2)]^+$ cation evolves ammonia ($m/z = 131.0$ Th), one or two H_2 molecules (peaks at $m/z = 129.0$ and 127.0 Th) and the fragment CH_2NH_2 ($m/z = 118.0$ Th). It is worth noting that this channel also generates $[\text{Ni}(\text{en})]^+$ ions, thus the dissociation according to eq 6 might compete with the subsequent expulsion of the $[\text{CH}_2\text{NH}_2]^+$ cation and the neutral CH_2NH_2 fragment.

It should be noted that several studies on the gas-phase fragmentation of nickel complexes with ethylenediamine have been reported. The gas-phase dissociation of the $[\text{Ni}(\text{en})_n]^{2+}$ ($n = 2$ to 5) species has been described by Schröder et al. Ligand evaporation was

observed for $n = 4, 5$ while inter-proton transfer processes occurred for $n = 3$. Remarkably, the gas-phase dissociation of the $[\text{Ni}(\text{en})_2]^{2+}$ dication occurs through intra-complex electron-transfer followed by charge separation to yield exclusively the $[\text{Ni}(\text{en})]^+$ cations and the non-detected $-^+$ as shown in eq 6 [18]. Our results indicate more complicated dissociation patterns for the $[\text{Ni}(\text{en})_2]^{2+}$ dication. These differences may be attributed to the different nature of the gas-phase generated species. In a previous study, the gas-phase $[\text{Ni}(\text{en})_2]^{2+}$ dication was generated by electrospraying millimolar solutions of ethylenediamine and NiCl_2 . Under these conditions, the (*trans*-1 Cl_2) compound could not be obtained from the above reagents in the solution as it is prepared by a reaction between $[\text{Ni}(\text{en})_3]^{2+}$ and a Ni(II) salt [38]. Therefore, the presence of a complex with two chelate ethylenediamine ligands is not evident, neither in solution nor in the gas-phase, and, consequently, the characteristic CID spectra could significantly differ from the data presented in this work.

ESI-MS and ESI-MS/MS of Encapsulated Dications $\{[\text{Cu}(\text{en})_2]@\text{cuc}[8]\}^{2+}$ ($2@\text{cuc}[8]^{2+}$) and $[\text{Cu}(\text{en})_2]^{2+}$ (2^{2+})

The ESI mass spectra of aqueous solutions of compound $\{\text{trans}-[\text{Cu}(\text{en})_2(\text{H}_2\text{O})_2]@\text{cuc}[8]\text{Cl}_2 \cdot 17\text{H}_2\text{O}\}$ also reveals the presence of a dication of formula $\{[\text{Cu}(\text{en})_2]@\text{cuc}[8]\}^{2+}$ ($2@\text{cuc}[8]^{2+}$) as the base peak, together with a set of triply charged ions assigned to the protonated, sodium and potassium adducts of general formula $[2@\text{cuc}[8] + \text{Y}]^{3+}$ ($\text{Y} = \text{H}, \text{Na}, \text{K}$). The ESI-MS of the compound $[\text{Cu}(\text{en})_2]\text{Cl}_2 \cdot 0.5\text{H}_2\text{O}$ shows abundant peak assigned to dicationic species of formula $[\text{Cu}(\text{en})_2]^{2+}$ (2^{2+}) along with the $[\text{Cu}(\text{en})_2 - \text{H}]^+$ and $[\text{Cu}(\text{en})_2 + \text{Cl}]^+$ cations. Analogously to the nickel [*trans*- $\text{Ni}(\text{en})_2\text{Cl}_2$] derivative, $[\text{Cu}(\text{en})_2 + \text{Cl}]^+$ and $[\text{Cu}(\text{en})_2]^{2+}$ prevail at low cone voltages ($U_c = 15$ V) while $[\text{Cu}(\text{en})_2 - \text{H}]^+$ was dominant at higher cone voltages (typically $U_c = 35$ V). The instrumental parameters required to generate maximum ion abundances of $2@\text{cuc}[8]^{2+}$ and 2^{2+} dications were identical to those used for the nickel analogues. The CID mass spectra of mass-selected $2@\text{cuc}[8]^{2+}$ are presented in Figure 4a at two representative collision energies $E_{\text{lab}} = 20$ (bottom) and 40 eV (top). The proposed fragmentation processes are described by eqs 8, 9, and 10.



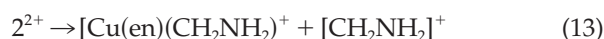
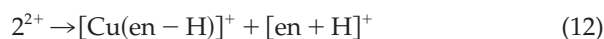
Similarly to its nickel analogue $\{1@\text{cuc}[8]\}^{2+}$, the $2@\text{cuc}[8]^{2+}$ dication shows coordination of one water molecule at low collision energies through ion-molecule reactions with background water available in the collision cell. At collision energies below 20 eV, $2@\text{cuc}[8]^{2+}$ shows a major fragmentation channel that includes the

loss of the neutral $(\text{en} - \text{H})$ fragment to give exclusively the species $\{\text{Cu}(\text{en})@\text{cuc}[8] + \text{H}\}^{2+}$ at $m/z = 726.2$ Th (eq 8). CID experiments using $d_4\text{-en}$ with deuterium atoms at the amine groups demonstrate that the proton loss arises from one of the amine groups (see Figure 4b). The most likely mechanism that accounts for this fragmentation consists of the intra-ligand proton transfer followed by electron-transfer from the deprotonated ethylenediamine to the copper site to produce neutral $(\text{en} - \text{H})$ and the $\{\text{Cu}(\text{en} + \text{H})@\text{cuc}[8]\}^{2+}$ dication at $m/z = 726.2$ Th. This fragmentation pathway closely resembles the ubiquitous dissociative intra-ligand proton transfer observed in most metal $[\text{ML}_2]^{2+}$ dications which bear protic ligands and produce $[\text{M}(\text{L} - \text{H})]^+$ and $[\text{L} + \text{H}]^+$ [30, 31], with the difference that the $[\text{en} + \text{H}]^+$ fragment is retained at the metal site while the neutral fragment $(\text{en} - \text{H})$ is released. Incidentally, other mechanisms such as the initial proton migration to the macrocycle cannot be definitively ruled out. Nevertheless, we admit that the simultaneous proton and electron-transfer observed in this case is unusual and, without theoretical support, the proposed mechanism remains merely speculative.

The increase of the collision energy results in two competitive channels that yield $\{\text{Cu}@\text{cuc}[8] + \text{H}\}^{2+}$ ($m/z = 696.1$ Th), through evaporation of one ethylenediamine molecule (eq 9), and afford $\{\text{Cu}@\text{cuc}[8]\}^+$ and $(\text{en} + \text{H})^+$ at $m/z = 1391.3$ and 61.1 Th, respectively (eq 10). At higher collision energies ($E_{\text{lab}} = 50$ eV), $\{\text{Cu}@\text{cuc}[8] + \text{H}\}^{2+}$ and $\{\text{Cu}@\text{cuc}[8]\}^+$ fragments following numerous pathways accompanied by attenuation of all ion signals. These results are in contrast with the rupture of the nickel $\{1@\text{cuc}[8]\}^+$ dication, in which well-defined expulsion of bis-N-methylene-glycoluril subunits has been observed.

The CID spectra of dication 2^{2+} are shown in Figure 5 together with the molecular composition of the detected product ions. Fragmentation starts at $E_{\text{lab}} = 10$ eV and reveals the presence of competitive pathways.

As observed for the nickel analogue, most of the product ions correspond to copper-containing species, with the metal atom coordinated to one of the organic ligands and/or a fragment of the ligand. Mass-selection and fragmentation of the less abundant ^{65}Cu -containing precursor isotopomer makes it possible to assign the copper-containing peaks. Eqs 11, 12 and 13 summarize the dissociation pathways observed.



The most intense fragmentation (eq 11) generates the cation $[\text{Cu}(\text{en})]^+$ ($m/z = 123.0$ Th) and, presumably, ionized ethylenediamine $-^+$ or some of its fragmentation products. This reaction is also observed for the 1^{2+} dication at higher collision energies. The observed dif-

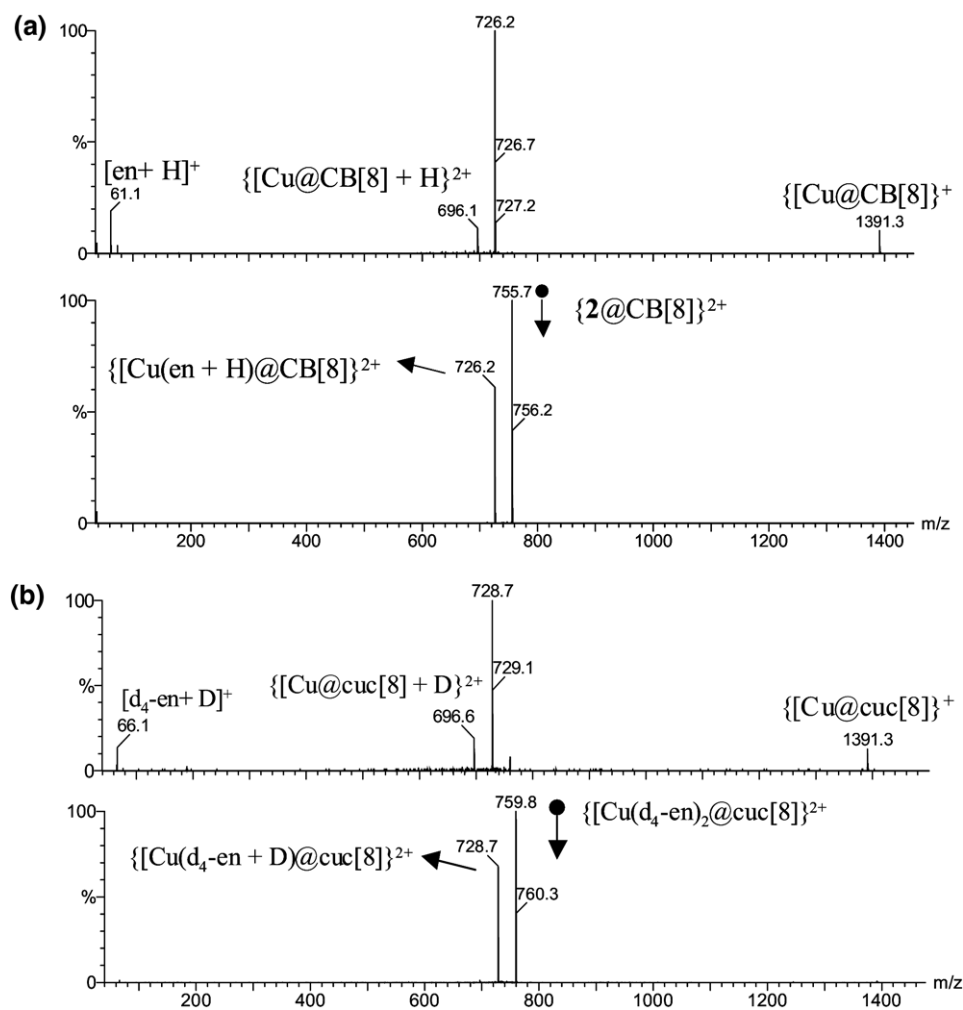


Figure 4. (a) Fragment ions formed upon CID at $E_{lab} = 20$ eV (bottom) and $E_{lab} = 40$ eV (top) of mass-selected $\{2@cuc[8]\}^{2+}$ dication at $m/z = 755.7$ Th and (b) mass-selected species $\{[Cu(d_4-en)_2@cuc[8]]\}^{2+}$ at $m/z = 759.8$ Th

ference may be attributed to the strongest tendency of the copper derivative towards reduction, in agreement with its higher second ionization energy. A second, minor channel (eq 12), associated with the inter-ligand

proton transfer accompanied by dissociation which produces $[Cu(en - H)]^+$ ($m/z = 122.0$ Th) and $[en + H]^+$ ($m/z = 61.1$ Th) species, is also observed. CID experiments using deuterated ethylenediamine

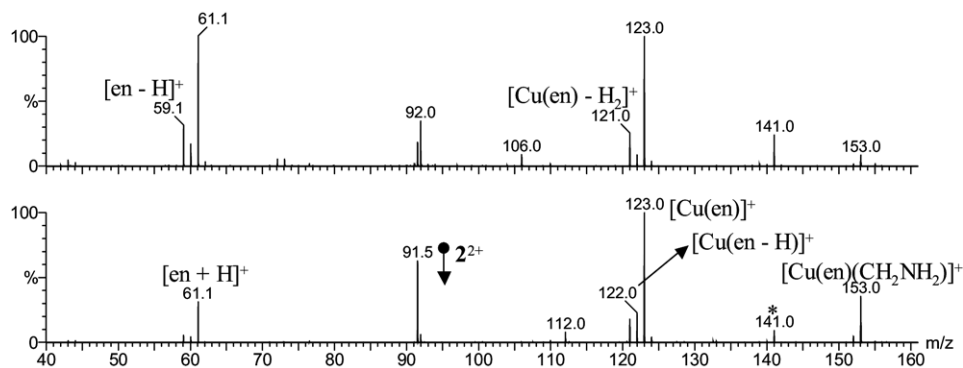


Figure 5. Fragment ions formed upon CID of mass-selected species 2^{2+} at $m/z = 91.5$ Th at $E_{lab} = 10$ eV (bottom) and $E_{lab} = 15$ eV (top). The peak marked with asterisk corresponds to product ions resulting from the bimolecular reaction with water: $*[Cu(en) + H_2O]^+$ at $m/z = 141.0$ Th

(ND₂CH₂CH₂ND₂ or d₄-en) were carried out to reveal that the proton loss takes place from one of the amine groups. It has to be pointed out that the relative intensities of the species appearing at $m/z = 61.1$ (eq 11) are higher than that at $m/z = 60.1$ (eq 12), despite the former corresponds to a minor fragmentation channel. This observation might be attributed to further fragmentation of the radical $-^+$ to afford species with lower mass-to-charge ratios or to a secondary reaction of the amine radical $-^+$ cation with background water present in the collision cell.

Again, one channel (eq 13) corresponds to the heterolytic carbon-carbon cleavage to give the [Cu(en)(CH₂NH₂)]⁺ cation at $m/z = 153.1$ Th. Further increase of the collision energy yields singly-charged species at $m/z = 121.0$, 106.0, and 59.1 Th. These product ions result from the loss of H₂, NH₃, and CuH from the [Cu(en)]⁺ cation. A prominent peak at $m/z = 92.0$ Th is also observed and tentatively assigned to the [Cu(CH₂ = NH)]⁺ species. To get deeper insight into its dissociation, mass-selection of the [Cu(en)]⁺ product ion was achieved by “in-source” fragmentation of 2²⁺ at $U_c = 60$ V. Its unimolecular dissociation generates species at $m/z = 121.0$, 106.0, 92.0, and 59.1 Th analogously to the species observed under identical conditions and previously described for 2²⁺. It should be noted that gas-phase generation of the [Cu(en)]⁺ cation has also been achieved using a chemical ionization-fast atom bombardment ion source and unimolecular dissociation of the cation was established by mass-analyzed ionic kinetic energy spectroscopy (MIKES) analysis [19]. Although the use of different techniques could result in distinctive fragmentation pathways [39], the results presented here closely resemble those previously reported by Alcamí et al., where a detailed description of the elementary steps involved was presented [19, 35].

The Effect of the Metal Nature on the Product Ions Observed Under CID

The development of electrospray ionization has facilitated considerably the access to gas-phase transition-metal complexes with oxidation states higher than 1+. Special attention is being paid to their gas-phase generation, gas-phase stability and dissociation features [40, 41]. In particular, the existence of several competitive processes in the gas-phase dissociation of solvated metal dications is well documented. For example, the gas-phase ion chemistry of the copper [Cu(H₂O)_n]²⁺ dications have been thoroughly investigated using different mass spectrometric techniques which indicate that the ligand loss and the proton and electron-transfer dominate in their CID spectra [42–45]. As shown above, the unimolecular dissociation studies of the dications 1²⁺ and 2²⁺ reveal a complex dissociation pattern due to intra-complex hydrogen and electron-transfer processes accompanied by C–C and C–N cleavages. While the nature of some of the fragments evolved could be assigned from deuterium labeling experiments and the

analysis of the isotopic pattern of the product ions, the intrinsic mechanism of the elementary steps involving such degradations is merely tentative without theoretical support.

Nevertheless, rich information can be extracted from the comparison of the dissociation pathways for the nickel 1²⁺ and {1@cuc[8]}²⁺ derivatives with those for their copper counterparts, 2²⁺ and {2@cuc[8]}²⁺. A common fragmentation channel observed for the 1²⁺ and 2²⁺ dications involves the heterolytic rupture of the organic ligand to afford a cation of general formula [M(en)(CH₂NH₂)]⁺ (M = Ni, Cu). In the case of the nickel species, a lower tendency for the formal reduction of the metal is observed. For example, the 1²⁺ dication mainly fragments through the inter-ligand proton migration (eq 4), hydride migration (eq 5) or heterolytic rupture of the organic ligand (eq 7), which formally do not represent a reduction of the Ni(II) metal. The reduced species such as [Ni(en)]⁺ or bare [Ni]⁺ are only observed at higher collision energies. In contrast, the CID spectra of the 2²⁺ dication are dominated by the reduced [Cu(en)]⁺ species. These experimental observations can be explained in terms of higher second ionization energies of the copper complexes that strongly favor the ligand-to-metal intra-complex electron-transfer. The same tendency is clearly seen while comparing the inclusion analogues: the metal in the {1@cuc[8]}²⁺ dication preserves its oxidation state under CID conditions, whereas the copper analogue appears formally reduced to Cu(I) in the species {[Cu(en)]@cuc[8] + H}²⁺, {Cu@cuc[8] + H}²⁺, and {Cu@cuc[8]}⁺. Of special interest is the distinctive fragmentation of the macrocycle upon CID of the {Ni@cuc[8]}²⁺ dications, in contrast with {CuH@cuc[8]}²⁺ and {Cu@cuc[8]}⁺. The nickel atom seems to play a crucial role in the expulsion of up to three bis-N-methylene-glycoluril subunits in well-defined ruptures which are not observed for the copper analogues. A tentative rupture scheme is proposed in Figure 2; the scheme implies up to four C–N ruptures mediated by the nickel atom. The mechanism for the formation of these product ions remains unclear.

The Effect of Metal Complex Encapsulation on the Product Ions Observed Under CID

The first remarkable observation is that the fragmentation channels typically observed for the free 1²⁺ and 2²⁺ dications (such as the [CH₂NH₂]⁺, H₂, [en – H]⁺, and NH₃ expulsion) are suppressed upon inclusion of the dications into the cucurbit[8]uril macrocycle; alternative ruptures are then accessed. Encapsulation into the cucurbit[8]uril macrocycle can modify the energetic barrier associated with such processes due to the presence of additional intermolecular interactions between the guest and the cucurbit[8]uril. These noncovalent interactions are mainly the combination of (1) ion-dipole interactions (between the positively charged

guest and carbonyl oxygens of the cucurbit[8]uril) and (2) hydrophobic interactions (between the guest and the inner surface of the cucurbit[8]uril host cavity) [7]. Any interaction in noncovalent complexes which compete with the solvent (e.g., ion-dipole) is greatly strengthened in the gas phase, while interactions such as hydrophobic forces are weakened. Therefore, the ion-dipole interactions represent the major contribution to the energetics of the encapsulated 1^{2+} and 2^{2+} guests in the gas phase.

The size effect of the free and encapsulated 1^{2+} and 2^{2+} complexes in the gas-phase must also be considered. In coordination complexes, as the number of ligands decreases (and so does the ion size), product ions resulting from the ligand-to-metal electron-transfer channels become predominant in their CID spectra, and for protic ligands intra-complex proton transfer processes appear to be competitive [31]. Both pathways, intra-complex ligand-to-metal electron-transfer and proton transfer processes, cause a charge reduction of the product ions. The presence of both processes is clearly distinguished in the characteristic dissociation of dications 1^{2+} and 2^{2+} where the presence of singly-charged product ions is dominant. Conversely, in the case of the larger inclusion species $\{1@cuc[8]\}^{2+}$ and $\{2@cuc[8]\}^{2+}$, the product ions are normally doubly-charged species. One plausible explanation of that would be the occupation of the vacant sites in the product ions resulting from the inclusion species $\{1@cuc[8]\}^{2+}$ and $\{2@cuc[8]\}^{2+}$ by the oxygen or nitrogen atoms of the macrocycle. In this way, charge alleviation in the guest complex through gas-phase host coordination could suppress charge reduction processes in complexes $\{1@cuc[8]\}^{2+}$ and $\{2@cuc[8]\}^{2+}$. In this context one could envision that the macrocycle acts to solvate and therefore stabilize higher charge states, analogously to that observed in the condensed phase. Even though this is fully applicable to the nickel analogue $\{1@cuc[8]\}^{2+}$, charge reduction is also observed at high collision energies ($E_{lab} = 50$ eV) for the copper $\{2@cuc[8]\}^{2+}$ dication. This experimental observation indicates that, for transition metals with high second ionization energies, an interplay of the effects of the ion size and the value of the second ionization energy governs their dissociation chemistry.

Let us note that size-effects related to the distinctive rates of unimolecular dissociation for the encapsulated and the smaller free metal complexes might also be invoked to account for the dissociation differences. The delayed dissociation typically observed for large ions is assumed to occur because their internal energy gets distributed over an increasing number of degrees of freedom and it is less sufficiently concentrated to produce the fragmentation [46, 47]. In this context, we consider feasible that for the larger molecules (such as $\{1@cuc[8]\}^{2+}$ or $\{2@cuc[8]\}^{2+}$ dications), there are more ways of partitioning the energy amongst its many modes and in consequence new dissociation pathways

different from that observed for the non-encapsulated complexes might become available.

Conclusions

The gas-phase generation of the 1^{2+} and 2^{2+} dications and their inclusion complexes with the cucurbit[8]uril macrocycle has been carried out by means of electrospray ionization. The unimolecular dissociation has been investigated by electrospray ionization tandem mass spectrometry. In all cases, bimolecular reactions with the background water present in the hexapole take place indicating that the metal site in species $[M(en)_2]^{2+}$ and $\{[M(en)_2]@CB[8]\}^{2+}$ ($M = Ni, Cu$) is easily accessible for coordination by neutral molecules. The nature of the metal (Ni or Cu) as well as the effect of encapsulation has a remarkable influence on the fragmentation pathways observed upon CID conditions. In the former case, the differences in the second ionization energies seem to heavily determinate the nature of the product ions. In particular, the copper-containing 2^{2+} and $\{2@cuc[8]\}^{2+}$ dications typically afford product ions with the metal reduced to Cu(I), while the product ions resulting from the nickel analogues, 1^{2+} and $\{1@cuc[8]\}^{2+}$, mainly preserve their $2+$ oxidation state. The effect of encapsulation also reveals a distinctive fragmentation of the 1^{2+} and 2^{2+} dications with respect to their cucurbit[8]uril-encapsulated counterparts. In this case, the restriction of the guest molecular mobility, mainly due to ion-dipole interaction with the cucurbit[8]uril macrocycle as well as the increased size of the encapsulated dications, results in distinctive fragmentation pathways.

Acknowledgments

The authors gratefully acknowledge financial support from the Ministry of Science and Technology of Spain (grant CTQ2005-09,270-C02-01), Generalitat Valenciana (grant ACOM/2007/286), the Bancaixa Castelló-UJI Foundation (grant P1-1B2001-07), and a grant from the Russian Academy of Sciences (program N7, Acad. A. I. Konovalov). The authors also thank the Servei Central D'Instrumentació Científica (SCIC) of the University Jaume I for providing them with the mass spectrometry facilities.

References

- Lebrilla, C. B. The Gas-Phase Chemistry of Cyclodextrin Inclusion Complexes. *Acc. Chem. Res.* **2001**, *34*, 653–661.
- Schafer, M. Supramolecular Crown Ether Adducts in the Gas Phase: From Molecular Recognition of Amines to the Covalent Coupling of Host/Guest Molecules. *Angew. Chem. Int. Ed.* **2003**, *42*, 1896–1899.
- Schalley, C. A.; Castellano, R. K.; Brody, M. S.; Rudkevich, D. M.; Siuzdak, G.; Rebek, J., Jr. Investigating Molecular Recognition by Mass Spectrometry: Characterization of Calixarene-Based Self-Assembling Capsule Hosts with Charged Guests. *J. Am. Chem. Soc.* **1999**, *121*, 4568–4579.
- Schalley, C. A. Molecular Recognition and Supramolecular Chemistry in the Gas Phase. *Mass Spectrom. Rev.* **2001**, *20*, 253–309.
- Vincenti, M.; Irico, A. Gas-Phase Interactions of Calixarene- and Resorcinarene-Cavitands with Molecular Guests Studied by Mass Spectrometry. *Int. J. Mass Spectrom.* **2002**, *214*, 23–36.
- Lee, J. W.; Samal, S.; Selvapalam, N.; Kim, S.-Y.; Kim, K. Cucurbituril Homologues and Derivatives: New Opportunities in Supramolecular Chemistry. *Acc. Chem. Res.* **2003**, *36*, 621–630.
- Lagona, J.; Mukhopadhyay, P.; Chakrabarti, S.; Isaacs, L. The cucurbit-[n]uril family. *Angew. Chem. Int. Ed.* **2005**, *44*, 4844–4870.

8. Kim, K.; Selvapalam, N.; Ko, Y. H.; Park, K. M.; Kim, D.; Kim, J. Functionalized Cucurbiturils and Their Applications. *Chem. Soc. Rev.* **2007**, *36*, 267–279.
9. Osaka, I.; Kondou, M.; Selvapalam, N.; Samal, S.; Kim, K.; Rekharsky, M. V.; Inoue, Y.; Arakawa, R. Characterization of host-guest complexes of cucurbit[n]uril ($n = 6, 7$) by electrospray ionization mass spectrometry. *J. Mass Spectrom.* **2006**, *41*, 202–207.
10. Kellersberger, K. A.; Anderson, J. D.; Ward, S. M.; Krakowiak, K. E.; Dearden, D. V. Cucurbit[6]uril pseudorotaxanes: Distinctive Gas-Phase Dissociation and Reactivity. *J. Am. Chem. Soc.* **2003**, *125*, 9284–9285.
12. Kim, S. Y.; Jung, Y. S.; Lee, E.; Kim, J.; Sakamoto, S.; Yamaguchi, K.; Kim, K. Macrocycles within Macrocycles: Cyclen, Cyclam, and Their Transition Metal Complexes Encapsulated in Cucurbit[8]uril. *Angew. Chem. Int. Ed.* **2001**, *40*, 2119–2120.
13. Mitkina, T. V.; Naumov, D. Y.; Gerasko, O. A.; Dolgushin, F. M.; Vicent, C.; Llusar, R.; Sokolov, M. N.; Fedin, V. P. Inclusion of Nickel(II) and Copper(II) Complexes with Aliphatic Polyamines in Cucurbit[8]uril. *Russ. Chem. Bull.* **2004**, *53*, 2519–2524.
14. Mitkina, T. V.; Naumov, D. Y.; Kuratieva, N. V.; Gerasko, O. A.; Fedin, V. P. Synthesis and Guest Exchange Reactions of Inclusion Compounds of Cucurbit[8]uril with Nickel(II) and Copper(II) Complexes. *Russ. Chem. Bull.* **2006**, *55*, 26–35.
15. Mitkina, T. V.; Sokolov, M. N.; Naumov, D. Y.; Kuratieva, N. V.; Gerasko, O. A.; Fedin, V. P. Jorgensen Complex Within a Molecular Container: Selective Encapsulation of $\text{Trans-[Co(en)}_2\text{Cl}_2\text{)]}^+$ into Cucurbit[8]uril and Influence of Inclusion on Guest's Properties. *Inorg. Chem.* **2006**, *45*, 6950–6955.
16. Chu, I. K.; Lau, T.-C.; Siu, K. W. M. Intraionic, Interligand Proton Transfer in Collision-Activated Macrocyclic Complex Ions of Nickel and Copper. *J. Mass Spectrom.* **1998**, *33*, 811–818.
17. Chaparro, A. L.; Vachet, R. W. Tandem Mass Spectrometry of Cu(II) Complexes: The Effects of Ligand Donor Group on Dissociation. *J. Mass Spectrom.* **2003**, *38*, 333–342.
18. Tsierekos, N. G.; Schröder, D.; Schwarz, H., Complexation of Nickel(II) by Ethylenediamine Investigated by Means of Electrospray Ionization Mass Spectrometry. *Int. J. Mass Spectrom.* **2004**, *235*, 33–42.
19. Alcamí, M.; Luna, A.; Mó, O.; Yañez, M.; Tortajada, J.; Amekraz, B. Unimolecular Reactivity of Strong Metal-Cation Complexes in the Gas-Phase: Ethylenediamine- Cu^+ . *Chem. Eur. J.* **2004**, *10*, 2927–2934.
20. Chu, I. K.; Rodriguez, C. F.; Hopkinson, A. C.; Siu, K. W. M.; Lau, T.-C. Formation of Molecular Radical Cations of Enkephalin Derivatives via Collision-Induced Dissociation of Electrospray-Generated Copper (II) Complex Ions of Amines and Peptides. *J. Am. Soc. Mass Spectrom.* **2001**, *12*, 1114–1119.
21. Chu, I. K.; Rodriguez, C. F.; Lau, T.-C.; Hopkinson, A. C.; Siu, K. W. M. Molecular Radical Cations of Oligopeptides. *J. Phys. Chem. B* **2001**, *104*, 3393–3397.
22. Wee, S.; O'Hair, R. A. J.; McFayden, W. D. Can Radical Cations of the Constituent of Nucleic Acids be Formed in the Gas Phase Using Ternary Transition Complexes. *Rapid Commun. Mass Spectrom.* **2005**, *19*, 1797–1805.
23. Barlow, C. K.; Moran, D.; Radom, L.; McFayden, W. D.; O'Hair, R. A. J. Metal-Mediated Formation of Gas-Phase Amino Acid Radical Cations. *J. Phys. Chem. A* **2006**, *110*, 8304–8315.
24. Barlow, C. K.; McFayden, W. D.; O'Hair, R. A. J. Formation of Cationic Peptide Radicals by Gas-Phase Redox Reactions with Trivalent Chromium, Manganese, Iron, and Cobalt Complexes. *J. Am. Chem. Soc.* **2005**, *127*, 6109–6115.
25. Lam, A. K. I.; Abrahams, B. F.; Grannas, M. J.; McFayden, W. D.; O'Hair, R. A. J. Tuning the Gas Phase Redox Properties of Copper(II) Ternary Complexes of Terpyridines to Control the Formation of Nucleobase Radical Cations. *Dalton Trans.* **2006**, 5051–5061.
26. Cuniff, J. B.; Vouros, P. False Positives and the Detection of Cyclodextrin Inclusion Complexes by Electrospray Mass Spectrometry. *J. Am. Soc. Mass Spectrom.* **1995**, *6*, 437–447.
27. Guo, M. Q.; Song, F.; Liu, Z.; Liu, S. Characterization of Noncovalent Complexes of Rutin with Cyclodextrins by Electrospray Ionization Tandem Mass Spectrometry. *J. Mass Spectrom.* **2004**, *39*, 594–599.
28. Franski, R.; Gierczyk, B.; Schroeder, G. Fragmentation and Skeletal Rearrangements of 2-Aryllylamino-5-Aryl-1,3,4-Oxadiazoles and Their Noncovalent Complexes with Cobalt Cation and Cyclodextrin Studied by Mass Spectrometry. *J. Mass Spectrom.* **2006**, *41*, 312–322.
29. Jayaweera, P.; Blades, A. T.; Ikonomou, M. G.; Kerbale, P. Production and Study in the Gas Phase of Multiply Charged Solvated or Coordinated Metal Ions. *J. Am. Chem. Soc.* **1990**, *112*, 2452–2454.
30. Shvartsburg, A. A.; Siu, K. W. Is There a Minimum Size for Aqueous Doubly Charged Metal Cations? *J. Am. Chem. Soc.* **2001**, *123*, 10071–10075.
31. Shi, T.; Siu, K. W.; Hopkinson, A. C. Fragmentation of Doubly Charged Metal-Acetamide Complexes: Second Ionization Energies and Dissociation Chemistries. *Int. J. Mass Spectrom.* **2006**, *255/256*, 251–264.
32. Shvartsburg, A. A.; Wilkes, J. G. Fragmentation Chemistry of DMSO Complexes of Metal Dications. *J. Phys. Chem. A* **2002**, *106*, 4543–4551.
33. Seto, C.; Stone, J. A. The reactions of $\text{Cu}^{2+}(\text{CH}_3\text{CN})_n$ ($n = 2-4$) and $\text{Cu}^{2+}(\text{CH}_3\text{CN})_3(\text{H}_2\text{O})$ at Low Collision Energy with Neutral Molecules in a Triple Sector Quadrupole Instrument. *Int. J. Mass Spectrom.* **1998**, *175*, 263–276.
34. Shvartsburg, A. A.; Wilkes, J. G.; Lay, J. O.; Siu, K. W. Fragmentation and Charge Transfer in Gas-Phase Complexes of Divalent Metal Ions with Acetonitrile. *Chem. Phys. Lett.* **2001**, *350*, 216–224.
35. Alcamí, M.; Luna, A.; Mó, O.; Yañez, M.; Tortajada, J. Theoretical Survey of the Potential Energy Surface of Ethylenediamine Plus Cu^+ Reactions. *J. Phys. Chem. A* **2004**, *108*, 8367–8372.
36. Kohler, M.; Leary, J. A. Gas-Phase Reactions of Doubly Charged Alkaline Earth and Transition Metal Complexes of Acetonitrile, Pyridine, and Methanol Generated by Electrospray Ionization. *J. Am. Soc. Mass Spectrom.* **1997**, *8*, 1124–1133.
37. Rogalewicz, F.; Hoppilliard, Y.; Ohanessian, G. Structures and Fragmentation of Zinc(II) Complexes of Amino Acids in the Gas Phase. I. Electrosprayed Ions Which are Structurally Different from their Liquid Phase Precursors. *Int. J. Mass Spectrom.* **1997**, *201*, 307–320.
38. State, H. M. Bis(Ethylenediamine)Nickel(II) Chloride. *Inorg. Synth.* **1960**, *6*, 198–199.
39. Rodriguez-Santiago, L.; Tortajada, J. Experimental and Theoretical Studies on the Gas Phase Reactivity of Formamide- Ni^+ Complexes Generated by FAB and Electrospray Ionization. *Int. J. Mass Spectrom.* **2002**, *219*, 429–443.
40. Stace, A. J. Metal Ion Solvation in the Gas Phase: The Quest for Higher Oxidation States. *J. Phys. Chem. A* **2002**, *106*, 7993–8005.
41. Schroder, D. Coulomb Explosions and Stability of Multiply Charged Ions in the Gas Phase. *Angew. Chem. Int. Ed.* **2004**, *43*, 1329–1331.
42. Stone, J. A.; Vukomanovic, D. Collisional Dissociation Studies of $\text{Cu}^{2+}(\text{H}_2\text{O})_n$ Using Electrospray Ionization Mass Spectrometry. *Int. J. Mass Spectrom.* **1999**, *185/186/187*, 227–229.
43. Stone, J. A.; Vukomanovic, D. Experiment Proves That the Ions $[\text{Cu}(\text{H}_2\text{O})_n]^{2+}$ ($n = 1, 2$) are Stable in the Gas Phase. *Int. J. Mass Spectrom.* **2001**, *346*, 419–422.
44. Blades, A.; Jayaweera, P.; Ikonomou, M. G.; Kebarle, P. Ion-Molecule Clusters Involving Doubly Charged Metal Ions M^{2+} . *Int. J. Mass Spectrom. Ion Processes* **1990**, *102*, 251–267.
45. Stace, A. J.; Walker, N. R.; Firth, S. $[\text{Cu}(\text{H}_2\text{O})_n]^{2+}$ Clusters: The First Evidence of Aqueous Cu(II) in the Gas Phase. *J. Am. Chem. Soc.* **1997**, *119*, 10239–10240.
46. Remacle, F.; Levine, R. D. Prompt and Delayed Dissociation of Energy-Rich Larger Molecules. *J. Phys. Chem. A* **1998**, *102*, 10195–10198.
47. Griffin, L. L.; McAdoo, D. J. The Effect of Ion Size on Rate of Dissociation: RRKM Calculations on Model Large Polypeptide Ions. *J. Am. Soc. Mass Spectrom.* **1993**, *4*, 11–15.